Vol. 554: 51–69, 2016
doi: 10.3354/meps11803

MARINE ECOLOGY PROGRESS SERIES
Mar Ecol Prog Ser

Published July 28

Increasing CO_2 changes community composition of pico- and nano-sized protists and prokaryotes at a coastal Antarctic site

Paul G. Thomson[1,2,*], Andrew T. Davidson[2,3], Lynsey Maher[2]

[1]School of Civil, Environmental and Mining Engineering and The UWA Oceans Institute, The University of Western Australia, Mailstop M470, 35 Stirling Highway, Crawley, Western Australia 6009, Australia

[2]Department of Sustainability, Environment, Water, Population & Communities, Australian Antarctic Division, Channel Highway, Kingston, Tasmania 7050, Australia

[3]Antarctic Climate and Ecosystems Cooperative Research Centre (ACECRC), University of Tasmania, Private Bag 80, Hobart, Tasmania 7001, Australia

ABSTRACT: Ocean acidification is a globally recognised phenomenon, but little is known of its impacts on Antarctic marine microbes. Here we report on the community response of pico- and nanophytoplankton, heterotrophic nanoflagellates (HNF) and prokaryotes (*Archaea* and *Bacteria*) to elevated CO_2 during 3 minicosm experiments over the 2008/2009 summer at Davis Station, Antarctica. Coastal seawater was incubated in 650 l minicosms (n = 6) for ≤12 d at CO_2 concentrations ranging from preindustrial levels to those predicted for 2100 and beyond. The abundance of pico- and nano-sized protists and prokaryotes were determined by flow cytometry, using chlorophyll autofluorescence to discriminate the phytoplankton, SYBR-Green to stain the prokaryotes and LysoTracker Green stain to discriminate the HNF. While the effects on nanophytoplankton abundance were inconclusive, our results show that increasing CO_2 can alter the composition of the microbial community in Antarctic coastal waters. Our 3 experiments consistently showed lower concentrations of HNF and higher abundances of picophytoplankton and prokaryotes in treatments exposed to elevated CO_2. While the mechanism remains to be confirmed, our study suggests that CO_2 may reduce the mortality of picoplankton by HNF grazing. Our results indicate that changes in the composition of Antarctic microbial communities may occur within the concentration range of 750 to 1118 ppm CO_2, potentially impacting the Antarctic food web through reduced food availability.

KEY WORDS: Ocean acidification · Minicosms · CO_2 · Flow cytometry · Picophytoplankton · Nanophytoplankton · Heterotrophic nanoflagellates · *Bacteria* · *Archaea*

INTRODUCTION

Ocean acidification is a well-recognised phenomenon (Caldeira & Wickett 2003). Atmospheric carbon dioxide (CO_2) concentrations currently around 400 ppm are predicted to reach 750 to 1000 ppm by the year 2100 (Raven et al. 2005, Raupach et al. 2007). As the world's oceans absorb up to one-third of the annual release of anthropogenic CO_2, surface water CO_2 concentrations have steadily increased, leading to a 30% increase in dissolved hydrogen ion (H^+) concentration since preindustrial times and a decrease in pH of approximately 0.1 unit (Raven et al. 2005). Under various CO_2 emission scenarios, surface water pH could decrease by at least 0.3 units by 2100 (Caldeira & Wickett 2005, Orr et al. 2005). These predictions of changes in ocean chemistry have led to international efforts to assess pos-

*Corresponding author: paul.thomson@uwa.edu.au

sible impacts on marine biota (SCOR/IOC Symposium Planning Committee 2004, Riebesell et al. 2010).

Marine microbes play a vital role in the world's oceans as they form the base of the marine food web, produce an estimated 50% of the world's oxygen and are involved in biogeochemical cycles that influence global climate (Legendre & Le Fèvre 1995, Hutchins et al. 2009). In the Southern Ocean, phytoplankton photosynthesis comprises up to 15% of all marine primary production on the earth (Huntley et al. 1991). Spring and summertime blooms of *Phaeocystis antarctica* and/or large diatoms drive this annual production against a background of nano- (2–20 µm) and pico-sized (0.2–2 µm) phytoplankton cells. Nanophytoplankton can contribute between 38 and 84% of the total autotrophic biomass in waters off east Antarctica (Davidson et al. 2010), while the picophytoplankton contribution is relatively low but may reach up to 33% (Wright et al. 2009).

The fate of this fixed carbon biomass is largely determined by the action of the microbial loop (Azam et al. 1983, 1991). Grazing by protozooplankton (20–200 µm) and heterotrophic nanoflagellates (HNF, 2–20 mm) can be the dominant source of phytoplankton and bacterioplankton mortality and can regulate the abundance, size structure and species composition of their prey (Froneman & Perissinotto 1996, Calbet & Landry 2004). When small, nano-sized phytoplankton are most abundant, grazing by HNF is enhanced and can account for up to 100% of the nanophytoplankton (Becquevort 1997, Froneman 2004, Calbet et al. 2008) and between 27 and 100% of bacterial production (Christaki et al. 2008, Pearce et al. 2010, Garzio et al. 2013). Bacteria are a major pathway for carbon flow in the Southern Ocean (Rivkin et al. 1996, Delille 2004), and their metabolism is critical for nutrient remineralisation and transforming dissolved organic carbon into bacterial biomass that supports bacterivores. In some oceans, bacteria can process up to 80% of the primary production and can contribute 40% of the planktonic carbon (Cho & Azam 1990, Ducklow et al. 1993, Azam 1998). Therefore, understanding how marine microbes may be affected by ocean acidification is important in predicting energy flow in future oceans.

Ocean acidification studies have revealed a range of responses by marine microbes. In phytoplankton, effects on calcification, photosynthesis, primary productivity, growth rates and nutritional value have all been recorded (Riebesell et al. 2000, Hare et al. 2007, Rossoll et al. 2012, Leu et al. 2013). However, responses can be species-specific and linked to cell physiology (Rost et al. 2008, Tortell et al. 2008, Berge et al. 2010, Trimborn et al. 2013). At a community level, it appears that increasing CO_2 can change the size structure and community composition of microbial communities, although results can be contradictory. Some studies have shown that exposure to higher CO_2 levels favours large diatoms (Tortell et al. 2008, Feng et al. 2010) while others have shown that pico- and/or nanophytoplankton can become dominant (Hare et al. 2007, Engel et al. 2008, Paulino et al. 2008, Meakin & Wyman 2011, Brussaard et al. 2013).

The effects on marine *Archaea* and *Bacteria* (here collectively called prokaryotes) are also unclear. Most studies report little or no effect of increasing CO_2 on their abundance (Grossart et al. 2006, Allgaier et al. 2008, Newbold et al. 2012, Roy et al. 2013) despite apparent changes in the composition of bacterial groups (Newbold et al. 2012, Roy et al. 2013, Sperling et al. 2013) and increases in bacterial production and enzymatic rates (Grossart et al. 2006, Feng et al. 2010, Piontek et al. 2010, Krause et al. 2012). While some effects are most likely caused directly by species-specific differences in CO_2 tolerance, indirect effects by changes in protozoan abundance, grazing rates and viral infection are also possible (Danovaro et al. 2011).

To date, most studies have found little effect on protozooplankton abundance or grazing rates. Aberle et al. (2013) found little effect on microzooplankton composition and diversity with increasing partial pressure of CO_2 (pCO_2) in mesocosm experiments in an Arctic fjord. In a Norwegian fjord, Suffrian et al. (2008) found no difference in microzooplankton community composition and grazing rates in mesocosms with up to 3× present-day atmospheric CO_2 levels. Only Rose et al. (2009) recorded any effect, finding an increased abundance of microzooplankton at elevated temperatures and CO_2 concentrations of 690 ppm in North Atlantic spring bloom water. In the Antarctic, to our knowledge only one study has shown an effect of elevated CO_2 on zooplankton, where krill had higher ingestion rates of microbes and excretion rates of ammonia, phosphate and dissolved organic carbon at approximately 672 ppm (Saba et al. 2012). We know of no studies on the effects of elevated CO_2 on HNF. Considering that grazing diverts 60 to 70% of carbon away from higher trophic levels and vertical flux (Froneman & Perissinotto 1996, Calbet & Landry 2004), increasing our understanding of the effects of ocean acidification on protozoan grazers will be important in understanding carbon flow in future oceans.

In this study, we report on the effects of enhanced CO_2 concentrations on the pico- and nanophytoplankton, HNF and heterotrophic marine prokaryotes from Antarctic coastal seawater.

MATERIALS AND METHODS

We performed 3 experiments using coastal seawater from offshore of Davis Station, Antarctica (68° 35′ S, 77° 58′ E). The experiments lasted up to 12 d and were performed between December 2008 and February 2009 in 650 l polythene tanks ('minicosms', n = 6) held in a temperature-controlled shipping container. Once filled, the tanks had an approximate 50 l headspace and were gas tight, except during periods of CO_2 manipulation and on sampling days. All minicosms were cleaned with Decon 90 (Decon Laboratories), followed by 10% analytical reagents (AR) grade HCl and rinsed with MilliQ water prior to each experiment. Following cleaning, the minicosms were rinsed by filling and draining with seawater before being filled with the microbial community that was incubated. Seawater was pumped to the minicosms from 2 m depth and 60 m offshore using a Teflon double-diaphragm pump fitted to a Teflon-lined hose. Mesh of 200 µm over the seawater intake excluded metazooplankton from the tanks. All 6 minicosms were filled simultaneously to ensure that they contained the same initial microbial community, and the contents were gently mixed by a shrouded auger rotating at 15 rpm. Seawater temperature in each tank was measured to ±0.01°C using platinum resistance thermometers (Guideline 9540) and maintained at ambient ±0.1°C by the container's refrigeration, offset against warming in each minicosm by 2 × 300 W aquarium heaters (Fluval) connected to a predictive temperature-control program via Carel temperature controllers.

Light was supplied to each minicosm by 2 HQI-TS metal halide lamps (150 W, Osram) at an average intensity of 200 µmol m^{-2} s^{-1} over a 19 h light:5 h dark cycle. The irradiance and photoperiod were chosen to reflect the prolonged period of twilight between November and February at Davis Station and changes in diel light cycles due to solar angle and mixed depth layers over summer in Antarctic waters (Smith et al. 2000, Thomson et al. 2008). Overall, the daily dose of photosynthetically active radiation (PAR) approximated 21% of the average downwelling surface irradiance at Davis Station around the summer solstice while the flux rate equated to ~50% of the daily noon-time clear-sky irradiance at 5 m depth at this site (Thomson et al. 2008).

Seawater carbonate chemistry

Seawater CO_2 manipulation and target concentrations followed recommendations in the Guide to Best Practices for Ocean Acidification (Gattuso et al. 2010, Riebesell et al. 2010). Carbonate chemistry methods are detailed in full by Davidson et al. (2016). At Davis Station, we used total alkalinity (TA) and pH to estimate carbonate chemistry during the dosing of our minicosms. Total alkalinity and total CO_2 (TCO_2) concentrations measured later from fixed samples in Australia were used to calculate our final treatment CO_2 concentrations. Total alkalinity was measured by open-cell potentiometric titration using a Metrohm 809 Titrando and single 800 Dosino auto-titrator (SOP 3b) (Dickson et al. 2007). Our estimates of total alkalinity at Davis Station were within 0.7% of TA standards (A. G. Dickson pers. comm.), and this offset was used to correct the measured alkalinity in minicosm samples.

The Mettler Toledo Easy Seven meter, calibrated on the National Bureau of Standards (NBS) pH scale using NBS buffers, measured seawater pH (SOP 6a; Dickson et al. 2007). CO2SYS.BAS (Lewis & Wallace 1998) was used to calculate pH of known TA and salinity (Dickson TA standards) that had been bubbled with nitrogen and pure CO_2 for ≥30 min. The pH meter was then manually calibrated to these samples at the calculated pH. The temperature of pH standards was measured using an NIST-calibrated Guideline 9540, 3 decimal place platinum resistance thermometer, and all pH measurements were performed in a closed vessel to avoid losses of aqueous CO_2.

Our field estimates of CO_2 were later confirmed by measurements made on samples returned to Australia. TCO_2 was determined by coulometry at the Commonwealth Scientific and Industrial Research Organisation (CSIRO) in Hobart following methods of Dickson et al. (2007). Our final CO_2 treatment concentrations were calculated using TA and TCO_2 concentrations at a precision of ±2 µmol l^{-1}.

Water samples for pH measurement and TCO_2 were collected using methods that minimised exposure to air. Samples were collected gently via a Teflon line with the end placed at the bottom of an acid-cleaned and MilliQ-rinsed 200 ml bottle. A small volume of the sample seawater was first used to rinse the bottle, and the bottle was then filled to overflowing and capped with a convex lid to exclude air. The pH was measured as soon as possible after the sample was obtained. Samples for TCO_2 were collected every second day into 250 ml bottles with convex caps to exclude air and were fixed with 100 µl of saturated solu-

Table 1. Experiment start dates, ambient seawater CO_2 concentrations at the time of collection and mean CO_2 concentrations (ppm) and pH values for the 6 treatments over the 3 experiments at Davis Station in the 2008–2009 summer. Mean CO_2 concentrations (Treat) are expressed as multiples of the global atmospheric CO_2 concentration of 385.54 ppm in December 2008 (http://co2now.org/). In Experiment 3, 3.2a× and 3.2b× designate treatments of similar mean CO_2 concentrations

Expt	Start date (dd/mm/yy)	Ambient CO_2 at collection (ppm)		CO_2 treatment					
				Tank 1	Tank 2	Tank 3	Tank 4	Tank 5	Tank 6
1	30/12/08	102	Treat:	0.2×	1.7×	3.3×	4.8×	5.0×	6.3×
			ppm:	84	643	1281	1848	1942	2423
			pH:	8.8	7.9	7.7	7.5	7.5	7.4
2	20/01/09	118	Treat:	0.3×	1.1×	2.0×	2.9×	3.0×	4.0×
			ppm:	120	406	754	1130	1162	1530
			pH:	8.6	8.1	7.9	7.7	7.7	7.6
3	09/02/09	232	Treat:	0.6×	1.2×	2.2×	3.2a×	3.2b×	4.4×
			ppm:	250	474	864	1240	1232	1711
			pH:	8.3	8.1	7.8	7.7	7.7	7.5

tion of mercuric chloride, kept cool and in the dark before being returned to Australia for later analysis.

Target CO_2 concentrations were reached by adding CO_2-saturated seawater. The volume required to reach the desired CO_2 concentration was calculated using CO2SYS.BAS software (Lewis & Wallace 1998). Coastal seawater in an acid-cleaned polythene drum was gravity fed and filtered through a 0.22 µm pore size AcroPak 500 cartridge filter (Pall) into another 20 l acid-cleaned drum and bubbled with CO_2 gas (BOC, food grade) for 1 h until saturated (as determined with a pH meter). To reach the required CO_2 targets, the CO_2 saturated water was added over approximately 2 h using medical infusion bags with intravenous drips to regulate flow rate. Thus, the introduction of CO_2 was as slow and gentle as possible to each of the tanks to minimise stress to the microbial community. Loss of CO_2 from solution in each tank due to photosynthetic draw-down of CO_2 by phytoplankton and loss of CO_2 to the headspace was quantified by daily measurements of carbonate chemistry and compensated for by adding further CO_2 saturated seawater to the tanks (as above).

Six treatments were established in each experiment to encompass atmospheric CO_2 concentrations from ambient to those predicted by the end of the 21st century (IPCC 2014) and beyond. Mean CO_2 values over the incubation periods were calculated and used to define the treatments as multiples of atmospheric CO_2 concentrations of 386 ppm measured at Mauna Loa Observatory in December 2008 (http://co2now.org/). For example, a mean of 1281 ppm equated to 3.3× CO_2. Treatment CO_2 concentrations ranged from ambient coastal seawater (<1×, at least 84 ppm) to approximately 4× CO_2 (1711 ppm). The exception was in the first experiment, which reached 6.3× or 2423 ppm (Table 1), equating to the maximum pCO_2 predicted by Caldeira & Wickett (2003).

Expts were designed to determine the effect of CO_2 on the microbial community rather than the ability of the microbes to mediate CO_2 concentrations. Thus, carbonate chemistry measurements were repeated daily, and additional CO_2-saturated seawater was added to each tank to maintain the target CO_2 concentrations during the minicosm incubations.

Minicosm incubations and sampling

Expts 1, 2 and 3 began on 30 December 2008 and on 20 January and 9 February 2009, respectively. Seawater for Expt 1 was collected 3 wk after the break out of land-fast sea ice, and for Expts 2 and 3, seawater was collected from open water interspersed with small, drifting ice floes. Day 0 samples were obtained prior to acidification; otherwise, samples were taken every second day until Day 10 in Expts 1 and 3 and Day 12 in Expt 2. Seawater samples were collected from taps located mid-tank for a suite of analyses including nutrients, chlorophyll *a* (chl *a*) and flow cytometry. An accompanying study on the microphytoplankton and protozooplankton can be found in Davidson et al. (2016). Total sample volumes removed during each experiment did not exceed 20% of the initial seawater volume.

Chl *a* analysis

A known volume of up to 1 l of seawater from each minicosm was filtered through 13 mm GF/F filters and was stored in liquid nitrogen until transported to Australia. In Australia, the filters were stored at

–135°C in an ultralow freezer (Sanyo) until they were analysed within 7 mo. Pigments were extracted, analysed and quantified by HPLC in accordance with Wright et al. (2010). Net growth rates of chl *a* were calculated over days of exponential growth for each experiment using the equation $r = \log(N_t/N_0)/t$ (Landry et al. 1995), where r = apparent growth, N_t and N_0 are the concentrations on the day exponential growth ended and at time 0 (Day 0), respectively.

Nutrients

Fe-EDTA was added to each minicosm at the beginning of each experiment to a final concentration of 5 nM to ensure ready availability and to overcome possible Fe limitation confounding the effects of increasing CO_2 concentrations. Macronutrients were not added to the treatments. Concentrations of nitrate and nitrite (NOx), phosphorus (P) and silica (Si) were determined by Analytical Services Tasmania, Department of Primary Industries, Parks, Water and Environment, Tasmanian Government. NOx and P were analysed using APHA Standard methods 4500-NO_3^-I and 4500-P G (2005), respectively, while Si was analysed using the APHA Standard method (2005) 4500-SiO_2 F (Eaton et al. 2006). Detection limits were 0.14 µM for NOx and P and 5.4 µM for Si.

Flow cytometry

Seawater samples for flow cytometry (FCM) were filtered through 50 µm mesh and kept refrigerated in the dark until analysed within 4 h. Samples for protist and prokaryotic abundance were analysed using FACScan and FACSCalibur (Becton Dickinson) flow cytometers, respectively, both fitted with 488 nm argon lasers. The sheath fluid used for protist analyses was 0.22 µm filtered seawater, while MilliQ water was used for prokaryotes. Samples were weighed to ±0.0001 g before and after each run to determine the volume analysed, and cell abundance was calculated using this volume and event counts from bivariate scatter plots. PeakFlow Green 2.5 µm beads (Invitrogen) were added to all samples as an internal size and fluorescent standard.

Pico- and nanophytoplankton

Fresh samples were housed in a beaker of ice while analysed for 5 to 10 min at a flow rate of approximately 60 µl min^{-1}. FCM phytoplankton populations were discriminated into regions in bivariate scatter plots of red chlorophyll autofluorescence (FL3) versus orange fluorescence (FL2). Populations were grouped into regions and analysed for relative cell size in bivariate scatter plots of side scatter (SSC) versus FL3 fluorescence, where a linear trend between cell size and chlorophyll autofluorescence has been previously demonstrated (Veldhuis et al. 1997).

HNF

LysoTracker Green (Invitrogen) is a weakly basic, amine probe that fluorescently stains the acidic food vacuole of marine heterotrophs (Johnson & Spence 2010). A working solution of LysoTracker Green was prepared daily by diluting the commercial stock 1:10 with 0.22 µm-filtered seawater. Ten ml of seawater from each treatment was stained with 7.5 µl of the working solution to give a final stain concentration of 75 nM and incubated in the dark and on ice for 10 min. Following incubation, a 1 ml sub-sample was transferred to a sterile 5 ml Falcon tube and run for up to 10 min at approximately 60 µl min^{-1}. LysoTracker Green-stained HNF were discriminated from phytoplankton and detrital particles in the sequence of scatter plots shown in Fig. 1 as described by Rose et al. (2004). Phytoplankton were identified based on their high chlorophyll autofluorescence versus forward scatter (Fig. 1a), and detrital particles were identified by their relatively high SSC (Fig. 1b). The 2.5 µm beads (Fig. 1c) were used for size estimation of the HNF after removal of the phytoplankton and detrital particles (Fig. 1d). Abundances from this technique have been found to be significantly and positively correlated against HNF counts by the standard DAPI epifluorescent microscopy technique in Antarctic waters by Thomson et al. (2010) and elsewhere by Rose et al. (2004) and Sintes & Del Giorgio (2010).

Flow cytometrically defined phytoplankton and HNF populations

Up to 4 regions of phytoplankton were identified in the bivariate scatter plots (Fig. 2a). Regions R1, R2 and R3 were evident in each experiment, while R4 was identified only in Expts 2 and 3. Cells of R1, R2 and R3 were characterised by low, moderate and high red (FL3) chlorophyll autofluorescence and low orange (FL2) autofluorescence. Cells of R4 were dis-

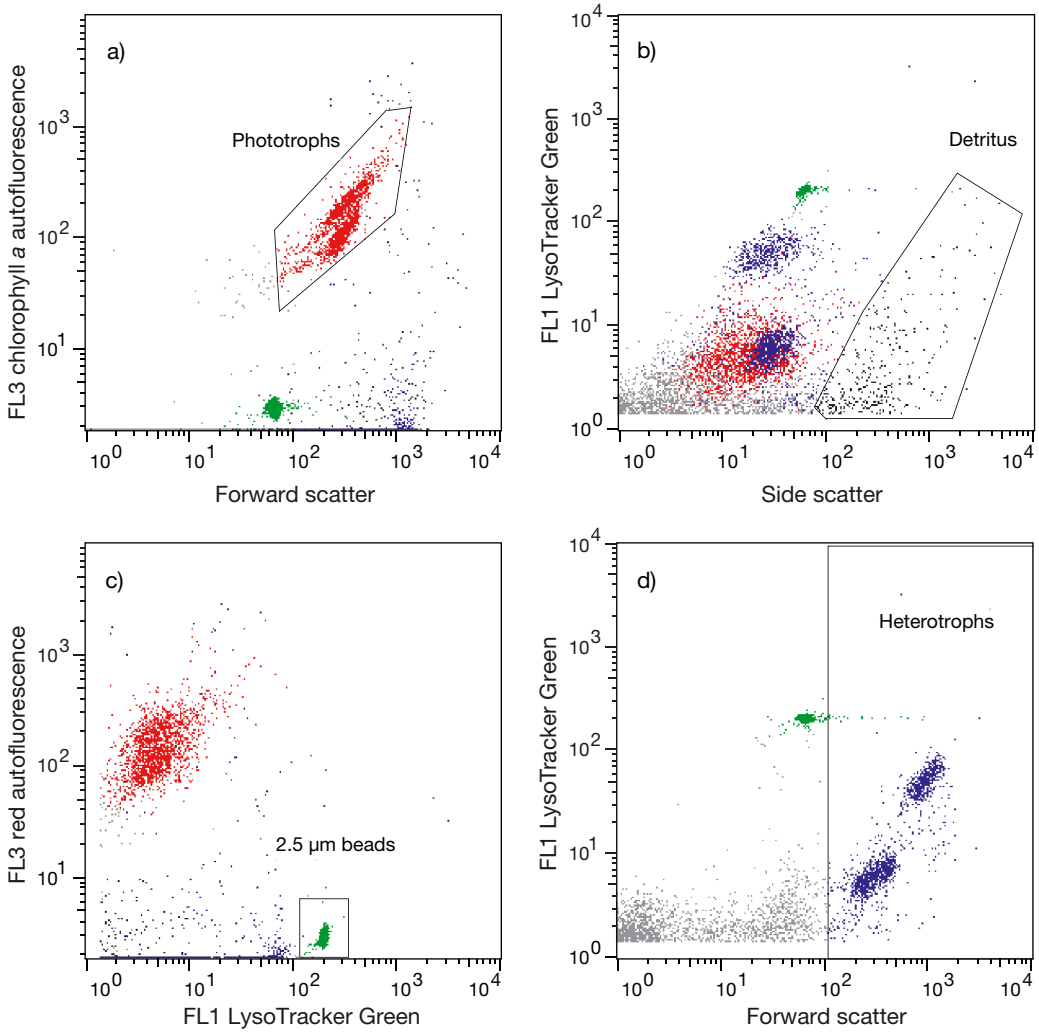

Fig. 1. Cytometric analysis of a LysoTracker Green-stained water sample for heterotrophic nanoflagellate abundance from Expt 1. (a) Phytoplankton were distinguished from other particles by their high red chlorophyll autofluorescence. (b) Detrital particles were identified based on their relatively high side scatter versus LysoTracker Green fluorescence. (c) Beads were identified by their high green versus low red fluorescence. (d) Populations in plots (a) and (b) were removed from the LysoTracker Green fluorescence and forward scatter plot and the remaining particles larger than 2.5 µm were counted as heterotrophic nanoflagellates (beads left in this plot only as a size indicator)

tinguished by moderate to high red chlorophyll autofluorescence and high orange autofluorescence, indicating that these cells were cryptophytes containing phycoerythrin. The lower sub-population in R4 most likely comprises smaller cryptophytes or those with lower chlorophyll autofluorescence. As the abundance of this sub-population rarely exceeded 100 cells ml^{-1} and was not always present, we did not separate these cells from others in this region.

The relative size of cells in each region was also estimated (Fig. 2b). Increasing chlorophyll autofluorescence with SSC indicated that relative size increased from the smallest in R1 through to the largest cells in R3 and R4 (cryptophytes), which appeared similar in size. Combined with the low chlorophyll autofluorescence and the relatively low SSC of cells of R1 compared to R2, it is likely that cells of R1 were picophytoplankton. Cells of R2 appeared to be smaller nanophytoplankton, as this region fell between the relative size range of the picophytoplankton (R1) and the cryptophytes (R4) by FL3 versus SSC. Cells of R3 were of equivalent size to the cryptophytes and were assumed to be the larger nanophytoplankton. Similar populations have resolved in other FCM studies in Antarctic and temperate waters (Larsen et al. 2001, Paulino et al. 2008). Populations of HNF stained with LysoTracker Green were most clearly defined in Expt 1, possibly due to high abundances of the choanoflagellate *Bicosta spinifera* (Fig. 1d) (Davidson et al. 2016).

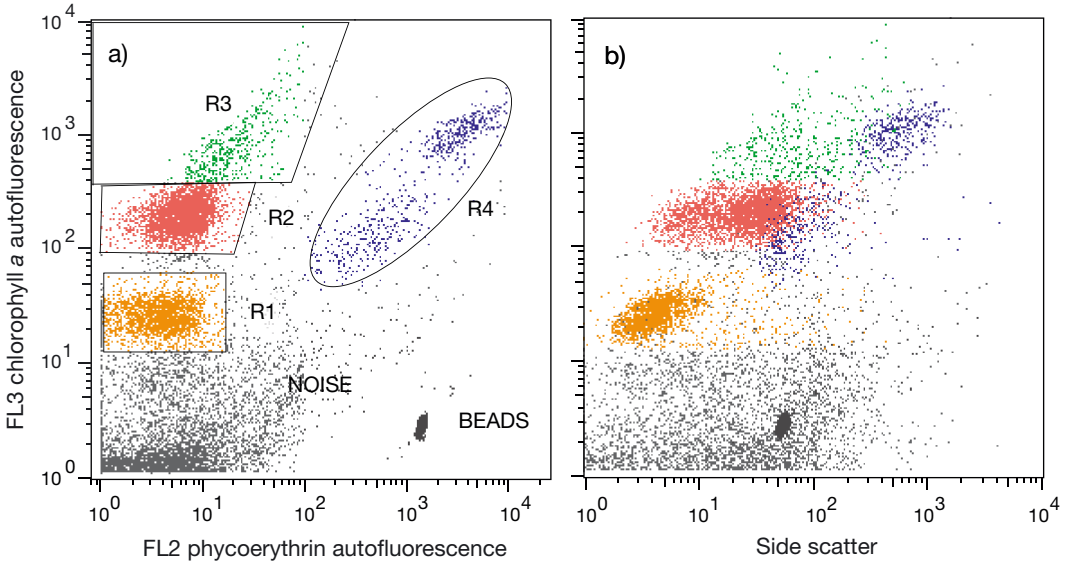

Fig. 2. Pico- and nanophytoplankton regions identified by flow cytometry. (a) Up to 4 regions (R) or populations of pico- and nanophytoplankton were discriminated based on their intensity of red (FL3) chlorophyll autofluorescence versus orange (FL2) phycoerythrin autofluorescence. (b) Using side scatter versus chlorophyll autofluorescence, we determined the relative sizes of the 4 regions and defined R1 as picophytoplankton and R2–R4 as nanophytoplankton. The high orange autofluorescence of R4 indicated that these cells were phycoerythrin-containing cryptophytes

Prokaryotes

The abundance of prokaryotes was determined from samples fixed to a final concentration of 0.5% glutaraldehyde for 1 h and stained for 20 min with 1:10 000 final dilution of SYBR-Green I (Invitrogen) (Marie et al. 2001). Samples were run for 3 min at a flow rate of approximately 35 µl min^{-1}. Total abundance was determined from bivariate scatter plots of SSC versus SYBR-Green I fluorescence (FL1).

Statistical analyses

Changes in community composition were analysed using the statistical package PRIMER v6.1.14 and PERMANOVA+ 1.0.4 (Clarke & Gorley 2006). Microbial abundances were $\log_{10}(x + 1)$ transformed and treated using the Gower metric similarity coefficient to give equal weighting among the microbes whose abundance varied over several orders of magnitude (e.g. prokaryotes and HNF).

Multi-dimensional scaling (MDS) plots were used to visualise changes in community composition within and among treatments over time (Clarke 1993). The location of each sample in the MDS reflected its community composition, and the distance between points indicated how similar (close) or different (far) the samples or communities were to each other. The line joining successive samples in each treatment shows the trajectory of change in community composition over time. Note that the fit of the ordination in a 2-dimensional space was measured by a stress factor, which in each experiment was ≤0.1. Stress values of ≤0.1 indicate a good ordination with little prospect of a misleading interpretation (Clarke 1993).

Two-way crossed permutational ANOVA (PERMANOVA, $\alpha = 0.05$, 999 permutations) was used to test for significant differences in community composition among treatments. Finally, cluster analysis and the similarity profile routine (SIMPROF, $\alpha = 0.05$ and 999 permutations; Clarke et al. 2008) was used to detect groups of samples that differed significantly. The different groups of samples obtained by SIMPROF were superimposed on the MDS plots as dashed ovals.

RESULTS

Seawater temperatures and salinities

Ambient seawater temperature and salinity were highest in Expt 1 at 1.63°C and 33.4 and decreased with the successive experiments, reaching −0.26°C and 33.1 in Expt 3 (Table 2). Mean water temperatures among treatments over the experimental period for each experiment were 1.54, 0.25 and −0.25°C, respectively, and differed little from the ambient temperatures at the time of collection. Salinity varied by ≤0.3 during the experiments.

Table 2. Ambient seawater temperatures and salinities at the time of water collection for incubations and mean experimental seawater temperatures and salinities for the 3 experiments

Expt	Ambient temp. (°C)	Ambient salinity	Mean (SD) experimental temp. (°C)	Mean (SD) experimental salinity
1	1.63	33.4	1.54 (0.24)	33.7 (0.01)
2	0.24	32.9	0.25 (0.11)	33.0 (0.26)
3	−0.26	33.1	−0.25 (0.07)	33.4 (0.03)

Ambient CO_2 and CO_2 treatments

Ambient coastal seawater CO_2 concentration at time of collection was 102, 118 and 232 ppm, respectively, for Expts 1, 2 and 3 (Table 1), equating to pH 8.6, 8.5 and 8.2. Such low ambient CO_2 concentrations due to biological draw-down have previously been reported near Davis Station during summer (Roden et al. 2013). Mean CO_2 and pH for each treatment in each experiment are given in Table 1. The pH values for the highest CO_2 treatments (≥4× CO_2) reached 7.4, 7.6 and 7.5 in Expts 1, 2 and 3, respectively. Full data on the carbonate chemistry in each of the treatments, including TA and TCO_2, are available in Table S1 in the Supplement at www.int-res.com/articles/suppl/m554p051_supp.pdf. Volumes of CO_2-saturated seawater added to each treatment to maintain the CO_2 target values throughout each experiment are shown in Table S2.

With the exception of treatment 1.7× CO_2 in Expt 1, concentrations in treatments with <2× CO_2 were relatively stable throughout the incubations (Fig. 3a–c). In contrast, fluctuations in CO_2 generally increased in magnitude with increasing CO_2 concentrations. This was particularly evident in Expt 1 between Days 4 and 6, when rates of CO_2 draw-down were high as chl *a* increased rapidly (see below).

Fluctuations in CO_2 concentrations were evident in most treatments in each experiment. Increases represented CO_2 addition to maintain target values, while decreases represented biological draw-down by phytoplankton and loss of CO_2 to an increasing volume of headspace in the tanks as the total seawater volume in each tank declined due to the removal of samples over time.

Chl *a*

Chl *a* increased to 5.6 and 6.4 µg l^{-1} in Expts 1 and 3, but in Expt 2 it remained relatively constant between 1 and 2 µg l^{-1} (Fig. 3d–f). In Expt 1, rapid increases in chl *a* were evident in all treatments, although concentrations in the 0.2× and 1.7× treatments were consistently highest to Day 8 (Fig. 3d). Apparent growth rates of chl *a* in the 0.2×, 1.7× and 3.3× CO_2 treatments were 0.38, 0.32 and 0.33 d^{-1}, respectively, but were lower (~0.24 d^{-1}) in treatments ≥4.8× CO_2. In Expt 3, chl *a* reached maximum concentrations by Days 4 or 6 and then declined by Day 10 (Fig. 3f). With the exception of the higher chl *a* concentrations in the lower CO_2 treatments in Expt 1, there was little discernible response of chl *a* to increasing CO_2. In Expt 3, apparent chl *a* growth rates to Day 6 were 0.12, 0.11 and 0.21 d^{-1} in the 0.6×, 1.2× and the 2.2× treatments, respectively, and consistently higher over the 10 d of incubation than those in treatments ≥3.8× CO_2 (~0.7 d^{-1}).

Nutrients

Despite filling the tanks simultaneously, nutrient concentrations sampled on Day 0 were variable, particularly in Expt 1 (Fig. 4). While the initial variation in nutrient concentrations could indicate that we sampled different water bodies while filling the tanks, coincident measurements of chl *a* and microbial abundance showed very little variability. Furthermore, microbial communities on Day 0 in each experiment showed no statistical difference in composition (see below). Instead, it is likely that the differences in nutrient concentrations were due to sampling low levels of suspended sediment in the tanks that had not settled and/or contamination during the sampling process. For example, the elevated nutrient concentrations in Expt 1 on Day 6 may be due to contamination, either of the nutrient samples themselves or of the CO_2 saturated seawater that was added to the minicosms to maintain the target CO_2 concentrations. While we concede that some of our nutrient data are not robust, the data do provide valuable information regarding the draw-down of nutrients and the time at which they became exhausted.

Expt 1

Nutrient concentrations were generally highest in Expt 1, with concentrations of NOx and P of at least 4.43 and 0.58 µM, respectively, on Day 0 (Fig. 4a,b). Both decreased with time to concentrations at or below detection levels (0.14 µM) by Day 10. There were no clear patterns among treat-

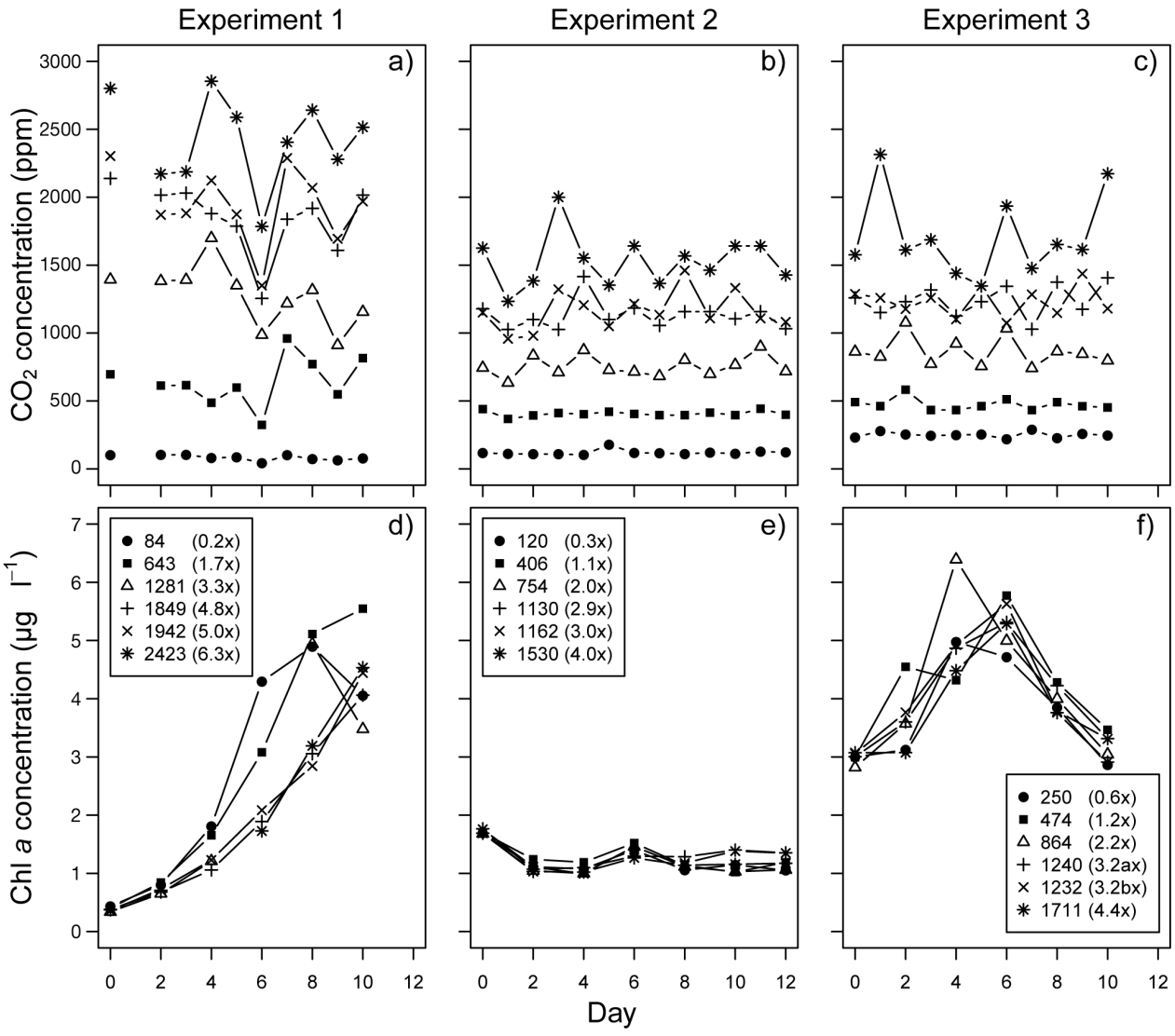

Fig. 3. (a–c) CO_2 and (d–f) chlorophyll *a* concentrations in each treatment in each experiment. Treatments are defined as mean CO_2 concentrations over each experiment and, in brackets, mean concentration expressed as multiples of the December 2008 atmospheric CO_2 concentration of 385.54 ppm (measured at Mauna Loa Observatory, http://co2now.org/)

ments, although from Day 6 onwards, concentrations of NOx and P were lowest in the 0.2× and 1.7× treatments.

Expt 2

Concentrations of NOx and P were persistently low in this experiment (Fig. 4d,e). NOx concentrations on Day 0 were detectable only in the 1.1×, 2.9× and 4.0× treatments at ≤0.43 µM and thereafter remained at or below the level of detection for all treatments. Concentrations of P were similarly low on Day 0 (≤0.29 µM) and with the exception of the 1.1× treatment were undetectable from Day 2.

Expt 3

Concentrations of NOx and P on Day 0 were considerably higher than those at the start of Expt 2 (Fig. 4g,h), indicating that either a different water mass had been advected to the collection point (see temperature and salinity differences in Table 2) or that the coastal water had experienced some nutrient regeneration between experiments. However, NOx concentrations were quickly depleted and were generally below detection levels by Day 6. Concentrations of P declined more slowly throughout the incubation but were generally depleted by Day 8.

Si concentrations were variable throughout each experiment, ranging between 32 and 107 µM (Fig. 4c,f,i).

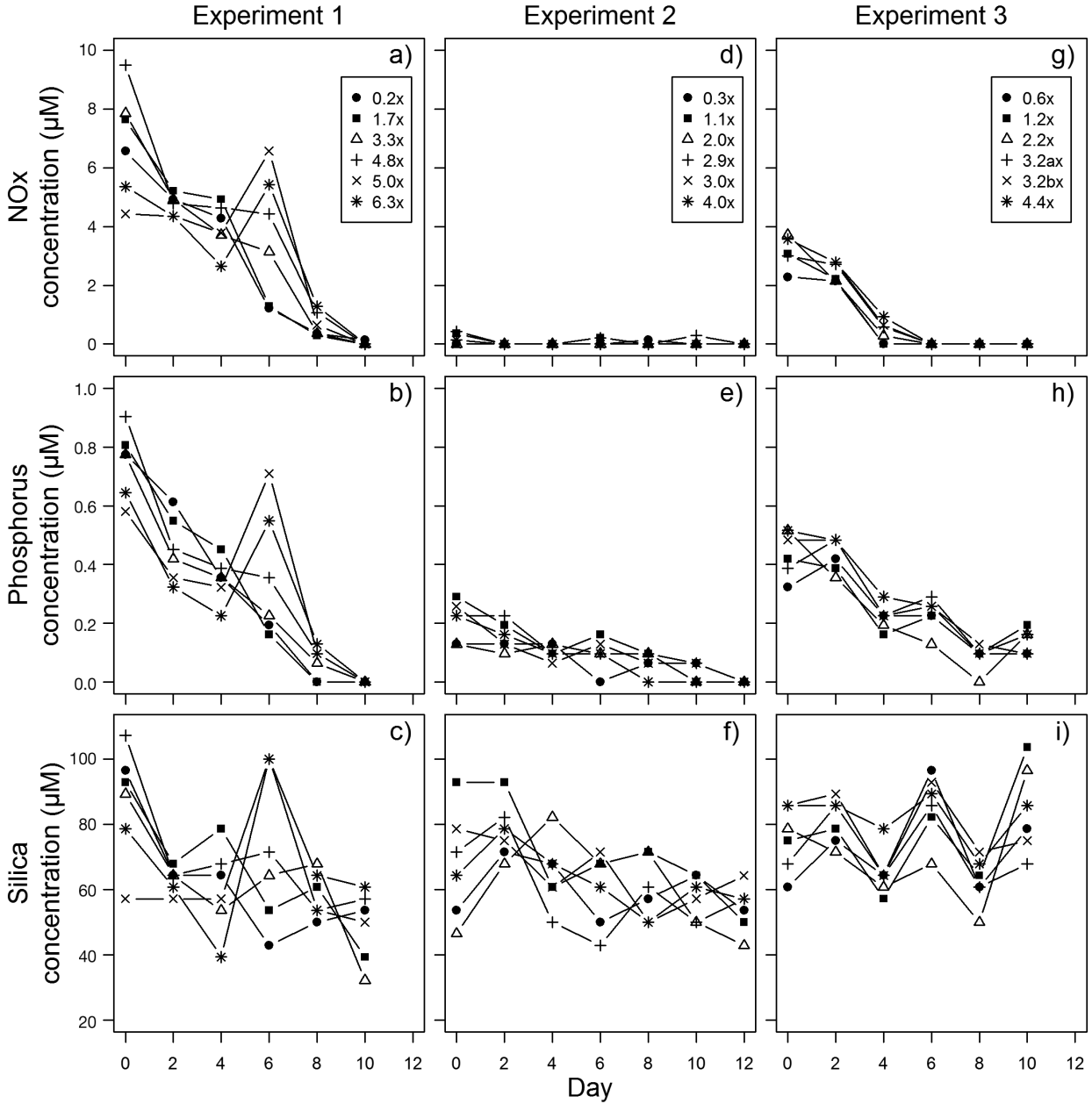

Fig. 4. Nutrient concentrations within each CO_2 treatment throughout each experiment: (a,d,g) nitrate and nitrite (NOx), (b,e,h) phosphorus and (c,f,i) silica. Treatments are as defined in Fig. 3

Only Expts 1 and 2 showed weak patterns of Si drawdown over time and were at no stage limiting to diatom growth.

Compared to another study at Davis Station at a nearby coastal site over summer, our initial NOx and P concentrations were low (cf. Gibson et al. 1997). Gibson et al. (1997) found NOx concentrations for December, January and February at approximately 20, 5 and 5 µM, and P concentrations of 1.5, 0.6 and 1.0 µM, respectively. Si concentrations were similar in both studies.

Effects of increasing CO_2 on marine microbes

Picophytoplankton

Picophytoplankton abundance was consistently greatest in high CO_2 treatments in each experiment while abundances in treatments ≤1.7× CO_2 in each experiment were consistently low (Fig. 5a–c). At ≈2× CO_2 in each experiment, abundances only slightly exceeded those of the lower treatments and generally followed the same pattern of growth. In

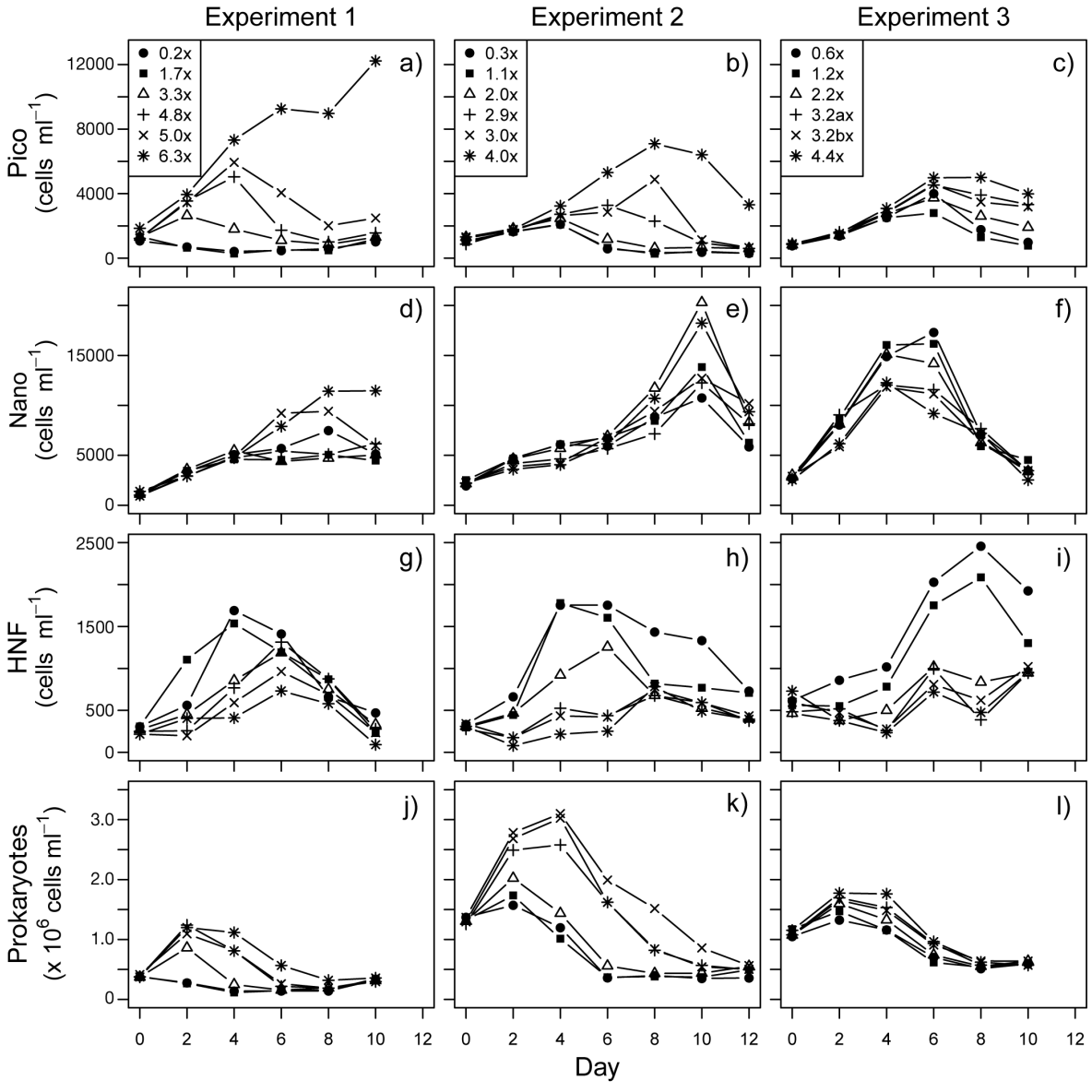

Fig. 5. Microbial abundance in the CO_2 treatments in each experiment, based on flow cytometry counts: (a–c) picophytoplankton, (d–f) nanophytoplankton, (g–i) heterotrophic nanoflagellates (HNF) and (j–l) prokaryotes in Expts 1, 2 and 3. Treatments are as defined in Fig. 3

contrast, the picophytoplankton were most abundant in the treatments ≥3× CO_2, where increases were evident to at least Day 4. Picophytoplankton in the highest treatment in Expt 1 were the exception, where abundances increased to Day 10.

Nanophytoplankton

Nanophytoplankton in R2 and R3 responded similarly to increasing CO_2, and their abundances were pooled. Overall, the effects on nanophytoplankton varied and were frequently unrelated to the CO_2 concentration (Fig. 5d–f). In Expt 1, abundances were commonly greatest in the 5.0× and 6.3× CO_2 treatments. Abundances in treatments exposed to ≤4.8× CO_2 remained low. In Expt 2, the abundance in all treatments peaked on Day 10, although this peak was highest in the 2× and 4× CO_2 treatments. Conversely, in Expt 3, nanophytoplankton abundance was highest in the lower treatments (≤1.2× CO_2) on Days 4 and 6, but progressively declined in CO_2 treatments >2.2× CO_2. Cryptophyte abundance was consistently low in Expts 2 and 3 (generally <1000 cells ml^{-1}, see Table S3 in the Supplement), showed no definitive

response to increasing CO_2 and are not considered further.

HNF

HNF abundance was highest in the lower CO_2 treatments (<2× CO_2) and decreased with increasing CO_2 on most days in all experiments (Fig. 5g–i). In Expts 1 and 2, HNF abundance in treatments ≤1.7 CO_2 peaked quickly by Day 4, reaching approximately 1700 cells ml^{-1}, thereafter declining to the end of the experiments. In Expt 3, abundance in treatments ≤1.2× CO_2 remained relatively low until Day 4, then increased quickly to reach at least 2000 cells ml^{-1} by Day 8. In contrast, HNF abundances in >2× CO_2 treatments were <1000 cells ml^{-1} and only increased slightly between Days 4 and 6, after which their numbers plateaued.

Prokaryotes

Like the picophytoplankton, prokaryotic abundances were consistently highest in treatments ≥2× CO_2 in all 3 experiments (Fig. 5j–l). Their abundances increased during the first 2 to 4 d of incubation, and then gradually declined. Prokaryotic abundance was lowest in Expt 1, highest in Expt 2 and moderate in Expt 3. In the first experiment, abundances in treatments ≥3.3× CO_2 at least doubled to around 1.0×10^6 $cells^{-1}$ ml^{-1} by Day 2 before decreasing over time. In Expt 2, abundances in the >2× CO_2 treatments increased rapidly in concentration to between 2.5 and 3.0×10^6 $cells^{-1}$ ml^{-1} by Day 4. In Expt 3, increases in abundance over the first 2 to 4 d were low, with the highest abundance (~1.7×10^6 $cells^{-1}$ $ml^{-}1$) in the highest CO_2 treatments.

Community-level responses

The effects we observed appeared independent of initial starting community type and nutrient availability. Expt 1 appeared to be a bloom-type community, as evidenced by rapidly increasing chl *a* concentrations and the rapid draw-down of nutrients. The community in Expt 2 appeared to be post bloom, with limiting nutrients throughout and low chl *a* concentrations. In the third experiment, the high initial prokaryotic concentration and moderate chl *a* and nutrient concentrations indicated that this was a community regenerating from recycled nutrients.

The relative abundance of microbes suggests possible community-level interactions. In particular, the lower numbers of HNF under higher CO_2 concentrations coincided with an increase in picophytoplankton and prokaryotic abundance. This was reflected in the trajectories of the treatments over time and their separation from each other (Fig. 6).

Overall, PERMANOVA showed significant differences among treatments in each experiment, and SIMPROF showed that the low CO_2 treatments (<2× CO_2) differed significantly from those at higher CO_2 (Fig. 6a–c and Figs. S1–S3 in the Supplement). There was no significant difference in community composition between treatments on Day 0 in any of the experiments (Figs. S1–S3).

Expt 1

PERMANOVA revealed a highly significant difference between the treatments with increasing CO_2 concentration and time (Treatment: pseudo-$F_{5,4}$ = 6.881, p = 0.002; Day: pseudo-$F_{4,5}$ = 23.419, p = 0.001), and SIMPROF demonstrated that this difference occurred between treatments exposed to ≤1.7× CO_2 and all higher CO_2 treatments (Fig. S1). Trajectories of the 0.2× and 1.7× CO_2 treatments advanced principally along Axis 1, and SIMPROF demonstrated that they were similar to each other throughout the experiment, with their community composition changing significantly between Days 0 and 2 and Days 2 and 4 but not changing markedly thereafter (Fig. 6a). In contrast, the trajectories of all higher treatments (≥3.3× CO_2) initially progressed along Axis 2, and these communities consistently differed in composition from those of the lower treatments after Day 0 (Fig. 6a). These communities were generally similar to each other and, though occasionally differing among times and treatments, culminated in a similar community after 6 and 8 d of incubation. The exception was the 6.3× CO_2 treatment.

Expt 2

PERMONVA results confirmed significant differences between the treatments (Treatment: pseudo-$F_{5,5}$ = 10.418, p = 0.001; Day: pseudo-$F_{5,5}$ = 27.440, p = 0.001). The trajectories of the communities over time and the grouping of samples in SIMPROF again showed significant differences in the composition of communities exposed to low (≤2.0× CO_2) and high (≥2.9× CO_2; Fig. 6b, Fig. S2). Trajectories of the 3 low

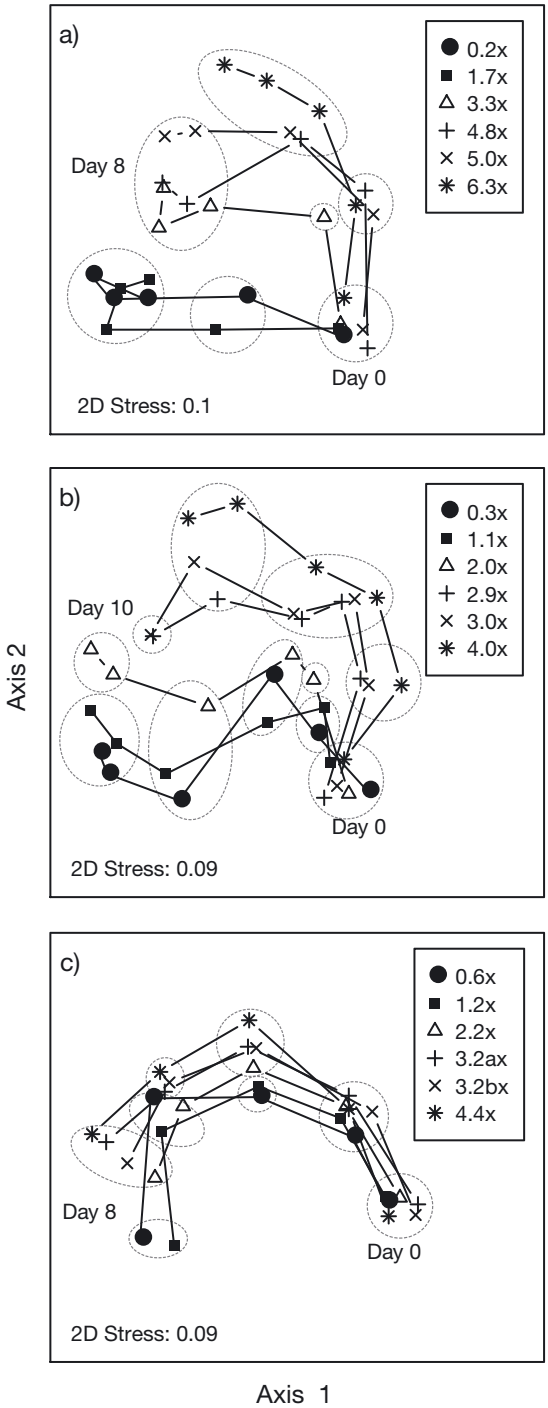

Fig. 6. Multidimensional scaling (MDS) plots mapping trajectories of change in communities of each CO_2 treatment in (a) Expt 1, (b) Expt 2 and (c) Expt 3. Trajectories extend from Day 0 to the day of maximum abundance of pico- and nanophytoplankton (Days 8, 10 and 8 for Expts 1, 2 and 3, respectively). Treatments are as defined in Fig. 3. The microbial communities of samples contained within a dashed oval do not differ significantly from each other but do differ from all other samples (SIMPROF, see Figs. S1–S3 in the Supplement at www.int-res.com/articles/suppl/m554p051_supp.pdf)

treatments progressed predominately along Axis 1, and SIMPROF results showed that these communities were generally similar in composition throughout the experiment, with the exception of the 2.0× CO_2 treatment on Days 2 and 10. Communities exposed to high CO_2 evolved principally along Axis 2, and their community composition was seldom different. However, these communities were clearly separated on all days and significantly differed from treatments exposed to ≤2.0× CO_2.

Expt 3

PERMANOVA results again indicated a highly significant difference in the response of microbes to increasing CO_2 and time (Treatment: pseudo-$F_{5,4}$ = 4.293, p = 0.002; Day: pseudo-$F_{4,5}$ = 76.156, p = 0.001). Unlike previous experiments, however, trajectories were generally similar but progressively changed along Axis 2 with increasing CO_2 concentrations and time (Fig. 6c). In this experiment, community composition was similar in all treatments until Day 4, when SIMPROF results identified significant differences in community composition between treatments ≤1.2× and those ≥3.2× CO_2 (Fig. S3). The 2.2× CO_2 community appeared as an intermediary, similar in composition to lower treatments on Day 6 but to the higher concentrations on other days (Days 4 and 8).

DISCUSSION

Our study describes the first minicosm-scale (650 l) ocean acidification experiments on marine microbial communities in Antarctic coastal waters. Other Antarctic studies have investigated the effects of elevated CO_2, although they used either small volumes (≤4 l) or continuous/semi-continuous batch incubations and reported only on the effects on phytoplankton or sea-ice algae (Tortell et al. 2008, 2010, Feng et al. 2010, Torstensson et al. 2012, McMinn et al. 2014). In the Arctic, larger-volume mesocosm studies have been performed with replicated treatments and macronutrient addition to stimulate microbial growth (Riebesell et al. 2008). We deliberately avoided macronutrient addition to allow us to determine the changing sensitivity of the microbial community over summer, including the effects of the draw-down and remineralisation of nutrients. In addition, we did not replicate our CO_2 treatments; instead, we opted for a larger range of CO_2 concentrations to increase the inferential power of our experiments and our ability to iden-

tify 'tipping points' in the microbial communities (Riebesell et al. 2010). In each experiment, we found that picophytoplankton and prokaryotic abundances increased at higher CO_2 concentrations and that this coincided with the inhibition of HNF abundance at $CO_2 \geq 750$ ppm. This result may reflect a reduction in the top-down control of the picophytoplankton and prokaryotes by HNF grazing.

We cannot discount that containment effects may have at least partially influenced our results, as they have in other mesocosm studies (Monier et al. 2014, Maugendre et al. 2015), despite our use of high volume tanks to minimise these effects. Typically, containment effects may include deviations of the incubated community from the natural community, reduced physical turbulence and wall effects (Sanford et al. 2001, Kim et al. 2008). Unfortunately, however, we lack replicates and samples that were not containerised to test these effects.

HNF

We are uncertain why higher CO_2 levels may have inhibited HNF. Invertebrate sperm can have reduced motility at approximately 1000 ppm CO_2, possibly resulting from the acidification of internal fluids and changes in ion balances, a decreased trans-membrane pH gradient and/or a reversal of motility activation signals in acidified water (Havenhand & Schlegel 2009, Morita et al. 2010). Modelling of near-organism H+ concentrations over a range of CO_2 concentrations shows that small cells (<5 µm), such as HNF, will experience higher concentrations of H+ in their thin boundary layers than larger cells in the same medium (Flynn et al. 2012). Thus, small HNF could be affected in similar ways to invertebrate sperm by increased acidity levels and perhaps are more vulnerable than the larger protozooplankton. However, the mechanism(s) leading to the inhibition of HNF abundance remain unknown, and future work is required to understand these effects on the physiology of small heterotrophic cells.

The inhibition of HNF abundance at CO_2 concentrations exceeding 750 ppm coincided with elevated abundances of picophytoplankton and prokaryotes. The HNF size spectrum overlaps that of their prey, and they can ingest up to 48% of daily phytoplankton production in the marginal ice zone (Becquevort 1997, Froneman 2004, Garzio et al. 2013). Nanoprotozoa are also well known bacterivores and can consume between 27 and 100% of bacterial production (Christaki et al. 2008, Pearce et al. 2010, Garzio et al. 2013). Thus, we suggest that the CO_2-induced inhibition of HNF at CO_2 concentrations ≥750 ppm released their prey from top-down control, resulting in the increased abundance of picophytoplankton and prokaryotes.

We are aware of no other studies showing inhibitory effects of increasing CO_2 on HNF abundance. All tanks were filled simultaneously and received the same physical and chemical conditions (other than CO_2), excluding such variations as an explanation for the lower HNF abundance. Nutrient concentrations were initially variable in Expts 1 and 3 but were not limiting to phytoplankton growth. Furthermore, SIMPROF results confirmed that there was no significance difference in community composition between the treatments on Day 0 in each experiment. Thus, differences in HNF abundance were not due to differences in initial microbial communities among minicosms at the start of the experiment. The greater variability of CO_2 concentrations in the higher treatments due to the lower buffering capacity of seawater at these levels may have somehow contributed to HNF inhibition. It is unknown, however, whether or how these fluctuations may affect HNF.

It is possible that our results were influenced by indirect effects of increasing CO_2 on other microbes and zooplankton that we did not measure. Viruses can control both bacterial and phytoplankton abundance through infection and cell lysis (Brussaard et al. 2013), and different viral classes may either be reduced in abundance or unaffected by increasing CO_2 (Larsen et al. 2001). Thus it is possible that the increased abundance of picophytoplankton and prokaryotes was due to a reduction in viral infection of these groups rather than a release from grazing pressure. Viral lysis may also have inhibited HNF abundance, although we are aware of no studies on viral infection of HNF.

We also have not accounted for the possible grazing by micro- and metazooplankton (20–200 and >200 µm, respectively) on HNF, picophytoplankton and prokaryotes. Microzooplankton (mainly dinoflagellates and ciliates) were observed in our experiments but did not differ significantly in concentration among treatments at ≤6 d incubation, and at no stage did they differ systematically in abundance with CO_2 (Davidson et al. 2016). Thus the microzooplankton are unlikely to be responsible for higher grazing mortality of HNF at high CO_2. The 200 µm mesh used to filter our seawater possibly allowed ingress of metazooplankton including small copepods and/or their nauplii that may also have affected abundances

through grazing. However, no metazooplankton were observed despite extensive microscopy of the minicosm samples. In addition, the consistency of our results over 3 experiments supports our conclusion that increasing CO_2 appeared to directly affect HNF abundance.

To our knowledge, no other study has found deleterious effects of increasing CO_2 concentration on HNF. The only research on protozoans we are aware of shows similar results to ours; proto- and microzooplankton are unaffected by increasing CO_2 concentrations up to 750–1000 ppm in Norwegian and North Atlantic waters (Suffrian et al. 2008, Rose et al. 2009, Aberle et al. 2013). Clearly, further studies are required to understand the effects of increasing CO_2 concentrations on protozoans.

Picophytoplankton

Other studies have also reported increased picophytoplankton abundance at CO_2 concentrations ≥700 ppm (Engel et al. 2008, Paulino et al. 2008, Meakin & Wyman 2011, Brussaard et al. 2013). Although they did not count HNF or measure grazing mortality, reduced grazing pressure was considered a possible explanation. Similarly to these studies, however, we cannot discount alternate hypotheses that include a complex interaction at the community level, including not only grazing and viral lysis (see above) but also size-dependent effects on nutrient and CO_2 uptake (Engel et al. 2008, Paulino et al. 2008, Meakin & Wyman 2011).

Nutrient concentrations appeared to have little effect on picophytoplankton growth and abundance. The large surface area to volume ratio of the picophytoplankton may have allowed them to effectively scavenge for macronutrients (Calder 2001) and continue multiplying. Furthermore, the picophytoplankton may also have effectively scavenged for Fe, the bioavailability of which can reportedly be reduced under increasing CO_2 (Shi et al. 2010). Finally, their small size and thin boundary layer (see above) may have been valuable in the higher CO_2 treatments in allowing concentrated CO_2 to accumulate close to the cell wall, benefiting the picophytoplankton via a ready supply of CO_2 and reduced metabolic energy in the production of carbon concentrating mechanisms (Raven et al. 2012). Overall, it is possible that reduced grazing pressure, the ability of smaller cells to compete for limited nutrients and access to plentiful CO_2 all contributed to their increased abundance at higher CO_2.

Nanophytoplankton

Like other studies, we found that the effects of increasing CO_2 on nanophytoplankton were less clear (Engel et al. 2008, Brussaard et al. 2013); nanophytoplankton were either unaffected by increasing CO_2 or showed inconclusive results (Expts 1 and 2). Only in Expt 3 did there appear to be an adverse effect of increasing CO_2, where nanophytoplankton were most abundant at lower CO_2 concentrations.

Prokaryotes

Our results indicate that prokaryotic abundances in Antarctic coastal waters may be enhanced at CO_2 concentrations ≥750 ppm, possibly reflecting reduced top-down control by CO_2-inhibited HNF. Alternatively, like the picophytoplankton, we cannot discount that the increased abundance of prokaryotes did not result from reduced viral lysis as a result of inhibited viral abundance at higher CO_2 (see above). Additionally, the increase in their abundance may result from a CO_2-related increased availability of dissolved organic carbon, a prokaryotic growth substrate. However, it is currently unclear how concentrations of dissolved organic carbon are affected by increasing CO_2 (Ray et al. 2012, MacGilchrist et al. 2014).

Our findings contrast with large-scale mesocosm studies that found no significant effect of increasing CO_2 on bacterial concentrations (Grossart et al. 2006, Allgaier et al. 2008, Newbold et al. 2012, Roy et al. 2013), despite findings that bacterial production and enzymatic rates are elevated at higher CO_2 concentrations (Grossart et al. 2006, Piontek et al. 2010). Differences in methodology may partially explain the contrasting results, where the mesocosm studies attained the CO_2 targets by bubbling seawater with CO_2 gas prior to the experiment. Seawater bubbling can strip communities of small fragile cells such as HNF and cause surface coagulation of organic matter (Engel et al. 2008). To our knowledge, only one other study has found higher prokaryotic abundances under enhanced CO_2. In that experiment, CO_2-saturated seawater was added gently using a 'spider' that injected and distributed the saturated water over depth during a Norwegian Fjord experiment (Riebesell et al. 2013, Endres et al. 2014). Thus, bubbling may adversely affect fragile HNF cells and growth substances across all treatments, resulting in a lack of discernible CO_2 effect on prokaryotic abundance.

Additionally, the mesocosm studies added macronutrients to stimulate phytoplankton blooms which can alter natural community composition and become the primary driver of community change in the mesocosms (Roy et al. 2013), masking the effects of increasing CO_2 on microbial communities (Riebesell et al. 2008). The Norwegian Fjord experiment showing enhanced bacterial abundance under higher pCO_2 further illustrates this effect over a 30 d incubation (Endres et al. 2014). In that experiment, nutrients were added after 13 d. Until this point, bacterial abundances had been increasing in all CO_2 treatments but at the greatest rate in the highest treatments. Following nutrient addition, bacterial abundance fell in the highest treatment as chl *a* concentrations increased dramatically. Bacterial abundances increased later to again show a CO_2 effect, but clearly, nutrient addition changed the dynamics of the microbes. Thus, nutrient addition appears to change the dynamics of the communities and may account for the contrast between our findings and those of previous studies.

Effects of increasing CO_2 on marine microbial communities

The community-level responses we observed were only evident from concentrations exceeding 750 ppm. Coastal environments undergo large pH fluctuations due to the input of snow and ice melt, and biological production and respiration (McNeil et al. 2011, Shadwick et al. 2013). At Davis Station, CO_2 can range between 100 and 420 ppm from mid-winter to late summer (Roden et al. 2013). Thus, coastal marine microbial populations appear to be already adapted to large variations in CO_2 and pH, which may partially explain the tolerance of the coastal microbes we measured to 750 ppm CO_2.

Our results indicate that increasing CO_2 concentrations may result in a change in the community composition and size structure of Antarctic coastal marine microbes. While we found that picophytoplankton abundance increased with CO_2, Davidson et al. (2016) found that in Expt 1, the abundance of larger phytoplankton decreased with CO_2 concentrations, particularly from 750 ppm. This change in size structure and species composition during a summer bloom community could have dire consequences for the Antarctic marine food web. For instance, blooms of large diatoms that drive Antarctic summer biological production may be susceptible under future CO_2 conditions predicted for the year 2100. Subsequently, higher trophic level animals may suffer from reduced food quality, quantity and size and key species in the food chain such as krill may have difficulty in harvesting cells <10 µm diameter (McClatchie & Boyd 1983). Furthermore, an increasing abundance of small, slow-sinking phytoplankton, together with increased bacterial abundance, would favour respiration of sequestered carbon in near-surface waters rather than sinking to depth, thereby reducing export efficiency.

Our study would have benefited from a range of rate measurements, particularly on the assessment of grazing rates. Microbial abundance reflects the dynamic equilibrium between growth and mortality. Inclusion of measurements of the size preference and rates of mortality due to grazing may have yielded further insights into the community responses we observed. In our experiments, the critical time points that influenced community composition occurred early in the incubations (≤6 d incubation). Thus, for future studies we recommend the incorporation of grazing dilution experiments timed to occur in the early stages of incubation.

Overall, results from our study suggest that increasing CO_2 may potentially result in changes in community composition of coastal Antarctic marine microbes. However, fully appreciating the impact of such changes will also require understanding other factors. For example, understanding the evolutionary potential of marine microbes to adapt to change will be critical to predicting the future effects of ocean acidification (Sunday et al. 2011), particularly as some species of microbes appear to be able to adapt to gradual changes in CO_2 concentrations over hundreds of generations (Langer et al. 2006, Lohbeck et al. 2012). Furthermore, understanding how ocean acidification affects metazooplankton will be crucial in determining overall effects on the Antarctic food chain. Other simultaneous stressors such as increasing seawater temperatures will act in synergy to affect marine microbes (Harvey et al. 2013). Future Antarctic studies should attempt to determine time scales of adaptability of species and to assess the combined effects of increasing CO_2 (ocean acidification), seawater temperature and other co-stressors (Boyd et al. 2008, Riebesell & Gattuso 2015).

Acknowledgements. This research was supported by AAS Project 40 and the Australian Antarctic Division (AAD). We gratefully acknowledge the assistance of S. Wright and R. van den Enden with pigment analyses and scanning electron microscopy work; Bronte Tilbrook and Kate Berry (supported by the Australian Climate Change Science Program) for the analysis of total dissolved inorganic carbon and total alkalinity at CSIRO Marine and Atmospheric Research Lab-

oratories in Hobart; AAD technical support in designing and equipping the minicosms; and Davis Station expeditioners in the summer of 2008–2009 for their support and assistance. We thank the reviewers for their comments that improved the manuscript. We acknowledge the facilities and the scientific and technical assistance of the Australian Microscopy & Microanalysis Research Facility at the Centre for Microscopy, Characterisation & Analysis, The University of Western Australia, a facility funded by the University, State and Commonwealth Governments.

LITERATURE CITED

Aberle N, Schulz KG, Stuhr A, Malzahn AM, Ludwig A, Riebesell U (2013) High tolerance of microzooplankton to ocean acidification in an Arctic coastal plankton community. Biogeosciences 10:1471–1481

Allgaier M, Riebesell U, Vogt M, Thyrhaug R, Grossart HP (2008) Coupling of heterotrophic bacteria to phytoplankton bloom development at different pCO_2 levels: a mesocosm study. Biogeosciences 5:1007–1022

Azam F (1998) Microbial control of oceanic carbon flux: the plot thickens. Science 280:694–696

Azam F, Fenchel T, Field JG, Gray JS, Meyer-Reil LA, Thingstad F (1983) The ecological role of water-column microbes in the sea. Mar Ecol Prog Ser 10:257–263

Azam F, Smith DC, Hollibaugh JT (1991) The role of the microbial loop in Antarctic pelagic ecosystems. Polar Res 10:239–244

Becquevort S (1997) Nanoprotozooplankton in the Atlantic sector of the Southern ocean during early spring: biomass and feeding activities. Deep-Sea Res II 44:355–373

Berge T, Daugbjerg N, Balling Andersen B, Hansen PJ (2010) Effect of lowered pH on marine phytoplankton growth rates. Mar Ecol Prog Ser 416:79–91

Boyd PW, Doney SC, Strzepek R, Dusenberry J, Lindsay K, Fung I (2008) Climate-mediated changes to mixed-layer properties in the Southern Ocean: assessing the phytoplankton response. Biogeosciences 5:847–864

Brussaard CPD, Noordeloos AAM, Witte H, Collenteur MCJ, Schulz K, Ludwig A, Riebesell U (2013) Arctic microbial community dynamics influenced by elevated CO_2 levels. Biogeosciences 10:719–731

Calbet A, Landry MR (2004) Phytoplankton growth, microzooplankton grazing, and carbon cycling in marine systems. Limnol Oceanogr 49:51–57

Calbet A, Trepat I, Almeda R, Saló V and others (2008) Impact of micro- and nanograzers on phytoplankton assessed by standard and size-fractionated dilution grazing experiments. Aquat Microb Ecol 50:145–156

Caldeira K, Wickett ME (2003) Oceanography: anthropogenic carbon and ocean pH. Nature 425:365

Caldeira K, Wickett ME (2005) Ocean model predictions of chemistry changes from carbon dioxide emissions to the atmosphere and ocean. J Geophys Res 110:C09S04, doi: 10.1029/2004JC002671

Calder WA (2001) Ecological consequences of body size. Encyclopedia of Life Sciences. John Wiley & Sons, Chichester

Cho BC, Azam F (1990) Biogeochemical significance of bacterial biomass in the ocean's euphotic zone. Mar Ecol Prog Ser 63:253–259

Christaki U, Obernosterer I, Van Wambeke F, Veldhuis M, Garcia N, Catala P (2008) Microbial food web structure in a naturally iron-fertilized area in the Southern Ocean (Kerguelen Plateau). Deep-Sea Res II 55:706–719

Clarke KR (1993) Non-parametric multivariate analyses of changes in community structure. Aust J Ecol 18:117–143

Clarke K, Gorley R (2006) PRIMER v6: user manual/tutorial. PRIMER-E, Plymouth

Clarke K, Somerfield PJ, Gorley RN (2008) Testing of null hypotheses in exploratory community analyses: similarity profiles and biota-environment linkage. J Exp Mar Biol Ecol 366:56–69

Danovaro R, Corinaldesi C, Dell'Anno A, Fuhrman JA, Middelburg JJ, Noble RT, Suttle CA (2011) Marine viruses and global climate change. FEMS Microbiol Rev 35: 993–1034

Davidson AT, Scott FJ, Nash GV, Wright SW, Raymond B (2010) Physical and biological control of protistan community composition, distribution and abundance in the seasonal ice zone of the Southern Ocean between 30 and 80°E. Deep-Sea Res II 57:828–848

Davidson A, McKinlay J, Westwood K, Thomson PG and others (2016) Enhanced CO_2 concentrations change the structure of Antarctic marine microbial communities. Mar Ecol Prog Ser 552:93–113

Delille D (2004) Abundance and function of bacteria in the Southern Ocean. Cell Mol Biol (Noisy-le-grand) 50: 543–551

Dickson AG, Sabine CL, Christian JR (2007) Guide to best practices for ocean CO_2 measurements. PICES Special Publication 3. North Pacific Marine Science Organization, Sidney, BC

Ducklow HW, Kirchman DL, Quinby HL, Carlson CA, Dam HG (1993) Stocks and dynamics of bacterioplankton carbon during the spring bloom in the eastern North Atlantic Ocean. Deep-Sea Res II 40:245–263

Eaton AD, Rice EW, Baird RB (eds) (2006) Standard methods for the examination of water and wastewater, Vol 2013. American Public Health Association. Available at www.standardmethods.org/

Endres S, Galgani L, Riebesell U, Schulz KG, Engel A (2014) Stimulated bacterial growth under elevated pCO_2: results from an off-shore mesocosm study. PLoS ONE 9: e99228

Engel A, Schulz KG, Riebesell U, Bellerby R, Delille B, Schartau M (2008) Effects of CO_2 on particle size distribution and phytoplankton abundance during a mesocosm bloom experiment (PeECE II). Biogeosciences 5:509–521

Feng Y, Hare CE, Rose JM, Handy SM and others (2010) Interactive effects of iron, irradiance and CO_2 on Ross Sea phytoplankton. Deep-Sea Res I 57:368–383

Flynn KJ, Blackford JC, Baird ME, Raven JA and others (2012) Changes in pH at the exterior surface of plankton with ocean acidification. Nat Clim Change 2:760

Froneman PW (2004) Protozooplankton community structure and grazing impact in the eastern Atlantic sector of the Southern Ocean in austral summer 1998. Deep-Sea Res II 51:2633–2643

Froneman PW, Perissinotto R (1996) Microzooplankton grazing and protozooplankton community structure in the South Atlantic and in the Atlantic sector of the Southern Ocean. Deep-Sea Res I 43:703–721

Garzio LM, Steinberg DK, Erickson M, Ducklow HW (2013) Microzooplankton grazing along the Western Antarctic Peninsula. Aquat Microb Ecol 70:215–232

Gattuso JP, Gao K, Lee K, Rost B, Schulz KG (2010) Approaches and tools to manipulate the carbonate chem-

istry. In: Riebesell U, Fabry VJ, Hansson L, Gattuso JP (eds) Guide to best practices for ocean acidification research and data reporting. Publications Office of the European Union, Luxembourg, p 41–52

Gibson JAE, Swadling KM, Burton HR (1997) Interannual variation in dominant phytoplankton species and biomass near Davis Station, East Antarctica. Proc NIPR Symp Polar Biol 10:77–89

Grossart HP, Allgaier M, Passow U, Riebesell U (2006) Testing the effect of CO2 concentration on the dynamics of marine heterotrophic bacterioplankton. Limnol Oceanogr 51:1–11

Hare CE, Leblanc K, DiTullio GR, Kudela RM and others (2007) Consequences of increased temperature and CO_2 for phytoplankton community structure in the Bering Sea. Mar Ecol Prog Ser 352:9–16

Harvey BP, Gwynn-Jones D, Moore PJ (2013) Meta-analysis reveals complex marine biological responses to the interactive effects of ocean acidification and warming. Ecol Evol 3:1016–1030

Havenhand JN, Schlegel P (2009) Near-future levels of ocean acidification do not affect sperm motility and fertilization kinetics in the oyster *Crassostrea gigas*. Biogeosciences 6:3009–3015

Huntley ME, Lopez MD, Karl DM (1991) Top predators in the Southern ocean: a major leak in the biological carbon pump. Science 253:64–66

Hutchins DA, Mulholland MR, Fu FX (2009) Nutrient cycles and marine microbes in a CO2-enriched ocean. Oceanography 22:128–145

IPCC (Intergovernmental Panel on Climate Change) (2014) Climate change 2014. Synthesis Report. Contribution of Working Groups I, II and III to the Fifth Assessment Report of the Intergovernmental Panel on Climate Change. IPCC, Geneva

Kim JM, Shin K, Lee K, Park BK (2008) In situ ecosystem-based carbon dioxide perturbation experiments: design and performance evaluation of a mesocosm facility. Limnol Oceanogr Methods 6:208–217

Krause E, Wichels A, Gimenez L, Lunau M, Schilhabel MB, Gerdts G (2012) Small changes in pH have direct effects on marine bacterial community composition: a microcosm approach. PLoS ONE 7:e47035

Johnson I, Spence MTZ (eds) (2010) Molecular probes handbook: a guide to fluorescent probes and labeling technologies, 11th edn. Life Technologies, Eugene, OR

Landry MR, Constantinou J, Kirshtein J (1995) Microzooplankton grazing in the central equatorial Pacific during February and August, 1992. Deep-Sea Res II 42:657–671

Langer G, Geisen M, Baumann KH, Kläs J, Riebesell U, Thoms S, Young JR (2006) Species-specific responses of calcifying algae to changing seawater carbonate chemistry. Geochem Geophys Geosyst 7:Q09006, doi:10.1029/GC001227

Larsen A, Castberg T, Sandaa RA, Brussaard CPD and others (2001) Population dynamics and diversity of phytoplankton, bacteria and viruses in a seawater enclosure. Mar Ecol Prog Ser 221:47–57

Legendre L, Le Fèvre J (1995) Microbial food webs and the export of biogenic carbon in oceans. Aquat Microb Ecol 9:69–77

Leu E, Daase M, Schulz KG, Stuhr A, Riebesell U (2013) Effect of ocean acidification on the fatty acid composition of a natural plankton community. Biogeosciences 10: 1143–1153

Lewis E, Wallace D (1998) Program developed for CO_2 system calculations. Carbon Dioxide Information Analysis Center, Oak Ridge National Laboratory, US Department of Energy, Oak Ridge, TN

Lohbeck KT, Riebesell U, Reusch TBH (2012) Adaptive evolution of a key phytoplankton species to ocean acidification. Nat Geosci 5:346–351

MacGilchrist GA, Shi T, Tyrrell T, Richier S, Moore CM, Dumousseaud C, Achterberg EP (2014) Effect of enhanced pCO_2 levels on the production of dissolved organic carbon and transparent exopolymer particles in short-term bioassay experiments. Biogeosciences 11:3695–3706

Marie D, Partensky F, Vaulot D, Brussaard C (2001) Enumeration of phytoplankton, bacteria, and viruses in marine samples. Current Protoc Cytom 10:11.11.11–11.11.15

Maugendre L, Gattuso JP, Louis J, de Kluijver A, Marro S, Soetaert K, Gazeau F (2015) Effect of ocean warming and acidification on a plankton community in the NW Mediterranean Sea. ICES J Mar Sci 72:1744–1755

McClatchie S, Boyd CM (1983) Morphological study of sieve efficiencies and mandibular surfaces in the Antarctic krill, *Euphausia superba.* Can J Fish Aquat Sci 40: 955–967

McMinn A, Müller MN, Martin A, Ryan KG (2014) The response of Antarctic sea ice algae to changes in pH and CO_2. PLoS ONE 9:e86984

McNeil BI, Sweeney C, Gibson JAE (2011) Natural seasonal variability of aragonite saturation state within two Antarctic coastal ocean sites. Antarct Sci 23:411–412

Meakin NG, Wyman M (2011) Rapid shifts in picoeukaryote community structure in response to ocean acidification. ISME J 5:1397–1405

Monier A, Findlay HS, Charvet S, Lovejoy C (2014) Late winter under ice pelagic microbial communities in the high Arctic Ocean and the impact of short-term exposure to elevated CO_2 levels. Front Microbiol 5:490

Morita M, Suwa R, Iguchi A, Nakamura M, Shimada K, Sakai K, Suzuki A (2010) Ocean acidification reduces sperm flagellar motility in broadcast spawning reef invertebrates. Zygote 18:103–107

Newbold LK, Oliver AE, Booth T, Tiwari B and others (2012) The response of marine picoplankton to ocean acidification. Environ Microbiol 14:2293–2307

Orr JC, Fabry VJ, Aumont O, Bopp L and others (2005) Anthropogenic ocean acidification over the twenty-first century and its impact on calcifying organisms. Nature 437:681–686

Paulino AI, Egge JK, Larsen A (2008) Effects of increased atmospheric CO_2 on small and intermediate sized osmotrophs during a nutrient induced phytoplankton bloom. Biogeosciences 5:739–748

Pearce I, Davidson AT, Thomson PG, Wright S, van den Enden R (2010) Marine microbial ecology off East Antarctica (30 – 80°E): rates of bacterial and phytoplankton growth and grazing by heterotrophic protists. Deep-Sea Res II 57:849–862

Piontek J, Lunau M, Händel N, Borchard C, Wurst M, Engel A (2010) Acidification increases microbial polysaccharide degradation in the ocean. Biogeosciences 7: 1615–1624

Raupach M, Marland G, Ciais P, Le Quéré C, Canadell JG, Klepper G, Field CB (2007) Global and regional drivers of accelerating CO_2 emissions. Proc Natl Acad Sci USA 104:10288–10293

Raven J, Caldeira K, Elderfield H, Hoegh-Guldberg O and

others (2005) Ocean acidification due to increasing atmospheric carbon dioxide. Policy Document 12/05. The Royal Society, London

Raven JA, Giordano M, Beardall J, Maberly SC (2012) Algal evolution in relation to atmospheric CO_2: carboxylases, carbon-concentrating mechanisms and carbon oxidation cycles. Philos Trans R Soc Lond B Biol Sci 367:493–507

Ray JL, Töpper B, An S, Silyakova A and others (2012) Effect of increased pCO_2 on bacterial assemblage shifts in response to glucose addition in Fram Strait seawater mesocosms. FEMS Microbiol Ecol 82:713–723

Riebesell U, Gattuso JP (2015) Lessons learned from ocean acidification research. Nat Clim Change 5:12–14

Riebesell U, Zondervan I, Rost B, Tortell PD, Zeebe RE, Morel FM (2000) Reduced calcification of marine plankton in response to increased atmospheric CO_2. Nature 407:364–367

Riebesell U, Bellerby RGJ, Grossart HP, Thingstad F (2008) Mesocosm CO_2 perturbation studies: from organism to community level. Biogeosciences 5:1157–1164

Riebesell U, Fabry VJ, Hansson L, Gattuso JP (eds) (2010) Guide to best practices for ocean acidification research and data reporting. Publications Office of the European Union, Luxembourg

Riebesell U, Czerny J, von Bröckel K, Boxhammer T and others (2013) Technical note: a mobile sea-going mesocosm system — new opportunities for ocean change research. Biogeosciences 10:1835–1847

Rivkin RB, Anderson MR, Lajzerowicz C (1996) Microbial processes in cold oceans. I. Relationship between temperature and bacterial growth rate. Aquat Microb Ecol 10:243–254

Roden NP, Shadwick EH, Tilbrook B, Trull TW (2013) Annual cycle of carbonate chemistry and decadal change in coastal Prydz Bay, East Antarctica. Mar Chem 155:135–147

Rose JM, Caron DA, Sieracki ME, Poulton N (2004) Counting heterotrophic nanoplanktonic protists in cultures and aquatic communities by flow cytometry. Aquat Microb Ecol 34:263–277

Rose JM, Feng Y, Gobler CJ, Gutierrez R, Hare CE, Leblanc K, Hutchins DA (2009) Effects of increased pCO_2 and temperature on the North Atlantic spring bloom. II. Microzooplankton abundance and grazing. Mar Ecol Prog Ser 388:27–40

Rossoll D, Bermudez R, Hauss H, Schulz KG, Riebesell U, Sommer U, Winder M (2012) Ocean acidification-induced food quality deterioration constrains trophic transfer. PLoS ONE 7:e34737

Rost B, Zondervan I, Wolf-Gladrow D (2008) Sensitivity of phytoplankton to future changes in ocean carbonate chemistry: current knowledge, contradictions and research directions. Mar Ecol Prog Ser 373:227–237

Roy AS, Gibbons SM, Schunck H, Owens S and others (2013) Ocean acidification shows negligible impacts on high-latitude bacterial community structure in coastal pelagic mesocosms. Biogeosciences 10:555–566

Saba GK, Schofield O, Torres JJ, Ombres EH, Steinberg DK (2012) Increased feeding and nutrient excretion of adult Antarctic krill, *Euphausia superba*, exposed to enhanced carbon dioxide (CO_2). PLoS ONE 7:e52224

Sanford A, Morgan J, Evans D, Ducklow H (2001) Bacterioplankton dynamics in estuarine mesocosms: effects of tank shape and size. Microb Ecol 41:45–55

SCOR/IOC (Scientific Committee on Oceanic Research/ Intergovernmental Oceanographic Commission) (2004) The ocean in a high CO_2 world. Oceanography Symposium Planning Committee 17:72–78

Shadwick EH, Rintoul SR, Tilbrook B, Williams GD and others (2013) Glacier tongue calving reduced dense water formation and enhanced carbon uptake. Geophys Res Lett 40:904–909

Shi D, Xu Y, Hopkinson BM, Morel FMM (2010) Effect of ocean acidification on iron availability to marine phytoplankton. Science 327:676–679

Sintes E, Del Giorgio PA (2010) Community heterogeneity and single-cell digestive activity of estuarine heterotrophic nanoflagellates assessed using lysotracker and flow cytometry. Environ Microbiol 12:1913–1925

Smith WO Jr, Marra J, Hiscock MR, Barber RT (2000) The seasonal cycle of phytoplankton biomass and primary productivity in the Ross Sea, Antarctica. Deep-Sea Res II 47:3119–3140

Sperling M, Piontek J, Gerdts G, Wichels A and others (2013) Effect of elevated CO_2 on the dynamics of particle-attached and free-living bacterioplankton communities in an Arctic fjord. Biogeosciences 10:181–191

Suffrian K, Simonelli P, Nejstgaard JC, Putzeys S, Carotenuto Y, Antia AN (2008) Microzooplankton grazing and phytoplankton growth in marine mesocosms with increased CO_2 levels. Biogeosciences 5:1145–1156

Sunday JM, Crim RN, Harley CDG, Hart MW (2011) Quantifying rates of evolutionary adaptation in response to ocean acidification. PLoS ONE 6:e22881

Thomson PG, Davidson AT, Cadman N (2008) Temporal changes in effects of ambient UV radiation on natural communities of Antarctic marine protists. Aquat Microb Ecol 52:131–147

Thomson PG, Davidson AT, van den Enden R, Pearce I, Seuront L, Paterson JS, Williams GD (2010) Distribution and abundance of marine microbes in the Southern Ocean between 30 and 80°E. Deep-Sea Res II 57:815–827

Torstensson A, Chierici M, Wulff A (2012) The influence of increased temperature and carbon dioxide levels on the benthic/sea ice diatom *Navicula directa*. Polar Biol 35: 205–214

Tortell PD, Payne CD, Li Y, Trimborn S and others (2008) CO_2 sensitivity of Southern Ocean phytoplankton. Geophys Res Lett 35:L04605, doi:10.1029/2007GL032583

Tortell PD, Trimborn S, Li Y, Rost B, Payne CD (2010) Inorganic carbon utilization by Ross Sea phytoplankton across natural and experimental CO2 gradients. J Phycol 46:433–443

Trimborn S, Brenneis T, Sweet E, Rost B (2013) Sensitivity of Antarctic phytoplankton species to ocean acidification: growth, carbon acquisition, and species interaction. Limnol Oceanogr 58:997–1007

Veldhuis MJW, Cucci TL, Sieracki ME (1997) Cellular DNA content of marine phytoplankton using two new fluorochromes: taxonomic and ecological implications. J Phycol 33:527–541

Wright SW, Ishikawa A, Marchant HJ, Davidson AT, van den Enden R, Nash GV (2009) Composition and significance of picophytoplankton in Antarctic waters. Polar Biol 32:797–808

Wright SW, van den Enden RL, Pearce I, Davidson AT, Scott FJ, Westwood KJ (2010) Phytoplankton community structure and stocks in the Southern Ocean (30–80°E) determined by CHEMTAX analysis of HPLC pigment signatures. Deep-Sea Res II 57:758–778

Editorial responsibility: Steven Lohrenz, New Bedford, Massachusetts, USA

Submitted: October 14, 2015; Accepted: June 14, 2016
Proofs received from author(s): July 13, 2016